The Ni-Ti-Zr System (Nickel-Titanium-Zirconium)

K.P. Gupta, The Indian Institute of Metals

Introduction

The Ni-Ti-Zr system has been studied in some detail in the 0 to 50 at.% Ni composition region, but only cursorily in the Ni-rich region. These studies established for the <50 at.% Ni region a pseudobinary section, one isopleth, and isothermal section, and the course of crystallization, and for the >50 at.% Ni region the phases existing along the 75 at.% Ni line.

Binary Systems

The Ti-Ni system [91Nas] (Fig. 1) shows three intermediate phases $TiNi_3$, TiNi, and Ti_2Ni of which the $TiNi_3$ and TiNi phases melt congruently at 1380 and 1310 °C, respectively, and the Ti_2Ni phase forms through a peritectic reaction L + TiNi ↔ Ti_2Ni at 984 °C. Three eutectic reactions—L ↔ γ + $TiNi_3$ (where γ is the fcc terminal solid solution of Ti in Ni), L ↔ $TiNi_3$ + TiNi, and L ↔ Ti_2Ni + βTi— occur at 1304, 1118, and 942 °C, respectively. The βTi solid solution undergoes a eutectoid reaction βTi ↔ αTi + Ti_2Ni at 765 °C. The TiNi phase is unstable below ~630 °C.

The Ni-Zr system [91Nas] (Fig. 2) has eight intermediate phases, Ni_5Zr, Ni_7Zr_2, Ni_3Zr, $Ni_{21}Zr_8$, $Ni_{10}Zr_7$, $Ni_{11}Zr_9$, NiZr, and $NiZr_2$, of which the Ni_7Zr_2, NiZr, and $NiZr_2$ phases melt congruently at 1440, 1260, and 1120 °C, respectively, whereas all the other phases form through peritectic or peritectoid reactions: L + Ni_7Zr_2 ↔ Ni_5Zr at 1300 °C, L + Ni_7Zr_2 ↔ $Ni_{21}Zr_8$ at 1180 °C, L + $Ni_{11}Zr_9$ ↔ $Ni_{10}Zr_7$ at 1160 °C, L + NiZr ↔ $Ni_{11}Zr_9$ at 1170 °C, Ni_7Zr_2 + $Ni_{21}Zr_8$ ↔ Ni_3Zr at 920 °C. Two eutectoid reactions, $Ni_{11}Zr_9$ ↔ NiZr + $Ni_{10}Zr_7$ and βZr ↔ αZr + $NiZr_2$, occur at 978 and 843 °C, respectively.

The Ti-Zr system [Massalski2] (Fig. 3) is an isomorphous system, for both liquid → solid and solid → solid reactions, with a solidus and liquidus minimum of 1540 °C at ~40 at.% Zr and a solid → solid transformation minimum of 605 °C at ~52 at.% Zr.

Binary and Ternary Phases

In the three binary systems Ni-Ti, Ni-Zr, and Ti-Zr systems, nine intermediate phases exist. In the Ni-Ti-Zr system, existence of two additional ternary intermediate phases have been reported: one around the $Ni_3(Ti_{66.7}Zr_{33.3})$ and the other around the NiTiZr composition regions. The phases existing in the binary and ternary system and their structure data are given in Table 1.

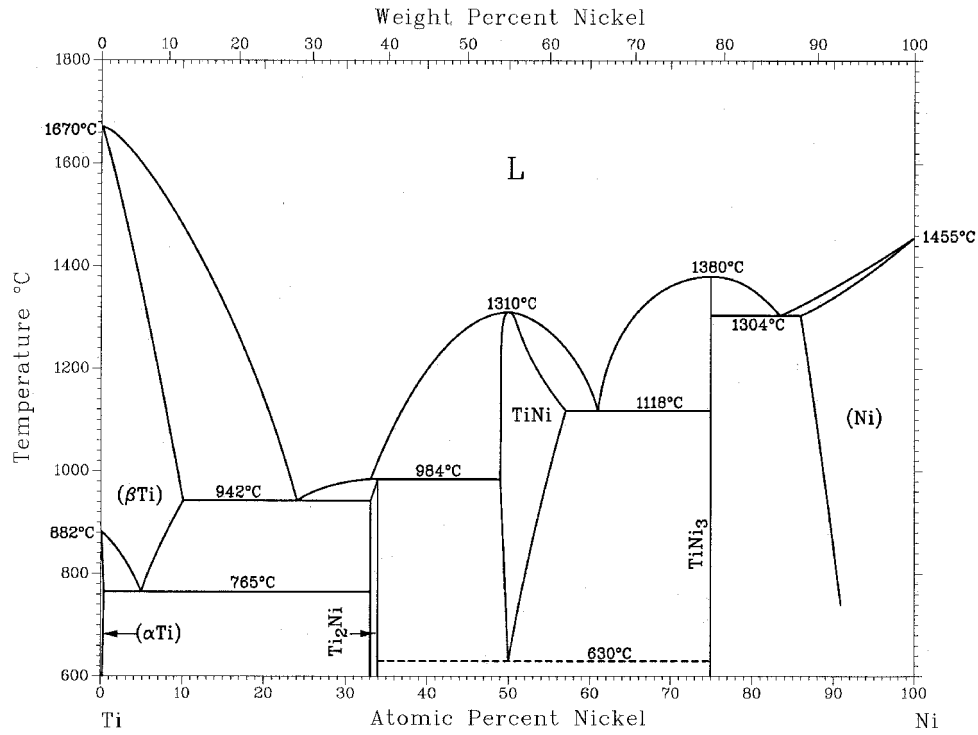

Fig. 1 Ti-Ni binary phase diagram [91Nas]

Ternary System

An exploratory study of the $Ni_3(Ti,Zr)$ alloys by [66Vuc] revealed the presence of a $BaPb_3$-type phase at the $Ni_3(Ti_{0.67}Zr_{0.33})$ composition. Since the new phase was found in the as-cast as well as in 1500 °C annealed state of the alloys and not at lower temperatures (<1300 °C), it was suggested that the phase at $Ni_3(Ti_{67}Zr_{33})$ composition exists only at high temperatures.

Table 1 Phases in binary Ni-Ti, Ni-Zr, Ti-Zr, and ternary Ni-Ti-Zr systems

Phase designation	Composition	Pearson symbol	Space group	Prototype	Lattice parameters, nm			Comment
					a	*b*	*c*	
(βZr, Ti)	…	*cI*2	$Im\bar{3}m$	W	…	…	…	…
(Ni)	…	*cF*4	$Fm\bar{3}m$	Cu	…	…	…	…
(αZr,Ti)	…	*hP*2	$P6_3/mmc$	Mg	…	…	…	…
ι	Ni_3Ti	*hP*16	$P6_3/mmc$	Ni_3Ti	0.5101	…	0.8307	…
β′	NiTi	*cP*2	$Pm\bar{3}m$	CsCl	0.3015	…	…	…
π′	$NiTi_2$	*cF*96	$Fd\bar{3}m$	CFe_3W_3	1.1324	…	…	…
ε	Ni_5Zr	*cF*24	$F\bar{4}3m$	$AuBe_5$	0.671	…	…	…
π	Ni_7Zr_2	*mC*36	*C*2/*m*	Ni_7Zr_2	0.4698	0.8235	1.2193	β = 95.83°
λ	Ni_3Zr	*hP*8	$P6_3/mmc$	Ni_3Sn	0.5309	…	0.4303	…
θ	$Ni_{21}Zr_8$	*aP*29	$P\bar{1}$	Hf_8Ni_{21}	0.6472	0.8065	0.8588	α = 75.19°; β = 68.04°; γ = 75.26°
β	$Ni_{10}Zr_7$	*oC*68(a)	*Aba*2	$Ni_{10}Zr_7$	0.9211	0.9156	1.2386	…
		*oP*68(b)	*Pbca*	$Ni_{10}Zr_7$	1.2497	0.9210	0.9325	…
ν	$Ni_{11}Zr_9$	*tI*40	*I*4/*m*	$Pt_{11}Zr_9$	0.990	…	0.662	…
φ	NiZr	*oC*8	*Cmcm*	CrB	0.3268	0.9936	0.4101	…
ξ	$NiZr_2$	*tI*12	*I*4/*mcm*	Al_2Cu	0.6483	…	0.5267	
T	$Ni_3(Ti_{0.67}Zr_{0.33})$	*hR*9	$R\bar{3}m$	$BaPb_3$	0.5157	…	1.8891	…
Ψ	NiTiZr	*hP*12	$P6_3/mmc$	$MgZn_2$	0.5200	…	0.8520	…

(a) Zr poor. (b) Zr rich

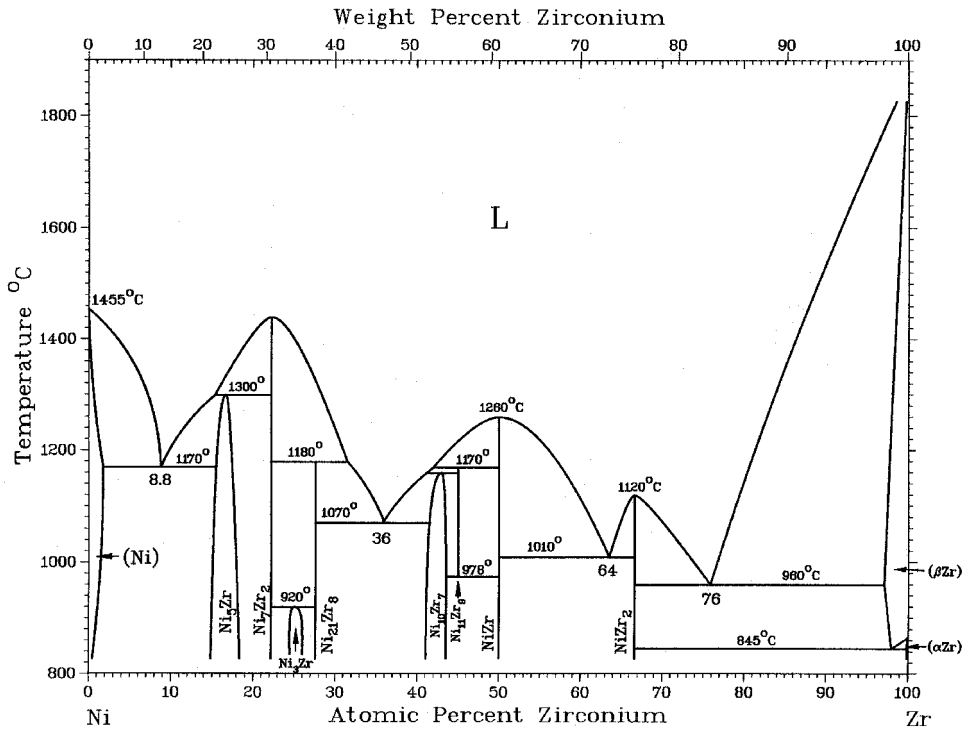

Fig. 2 Ni-Zr binary phase diagram [91Nas]

A more detailed investigation of the $Ni_3(Ti_xZr_{1-x})$ alloys was carried out by [87Gli]. The alloys were arc melted using component elements of 99.99 mass% purity and annealed at 900 °C for 180 h. Phase analysis was carried out using optical microscopy, x-ray diffraction (XRD), microhardness measurements, and a scanning electron microscope (SEM) fitted with an energy-dispersive analysis facility. Lattice parameters were used to find the phase boundaries of the Ni_3Ti and Ni_3Zr phases. This investigation showed that the two terminal solid solutions Ni_3Ti (ι) and Ni_3Zr (λ) extend into the ternary up to ~3.3 at.% Zr (Ni_3Ti to $Ni_3Ti_{0.87}Zr_{0.13}$) and ~1.5 at.% Ti (Ni_3Zr to $Ni_3Zr_{0.94}Ti_{0.06}$), respectively. An $Ni_3(Ti_xZr_{1-x})$ phase (T) of $BaPb_3$ type was found to exist at 900 °C between Ti contents of $0.60 \le x \le 0.70$ at.%. While the presence of $BaPb_3$-type phase was confirmed by [87Gli], the temperature range of stability of this phase was found to be much lower than reported by [66Vuc]. Two eutectic or eutectoid-type microstructures were observed at near 75 at.% Ni and 5 at.% Ti between the ι and T phase regions, and near 75 at.% Ni and between 17.5 and 20 at.% Ti, between the T and Ni_3Ti(λ) phase regions.

Pseudobinary

[90Ere] used 14 arc melted Ni(Ti,Zr) alloys to establish a peritectic-type pseudobinary diagram between the NiTi(β′) and NiZr(ϕ) phases. Differential thermal analysis (DTA) was used to determine the solid → liquid transition temperatures and alloys were annealed between 700 and 1300 °C for 8 to 125 h (depending on annealing temperature) and used to determine phase boundaries by means of XRD, microscopy, and local x-ray spectroscopic analysis (EPMA). A peritectic reaction L + NiZr ↔ NiTi was found to occur at 1160 °C at ~46 at.% Zr. In the L + NiTi(β′) two-phase region a solidus-liquidus minimum of 1100 °C was reported to occur at ~25 at.% Zr (Fig. 4).

Isopleth

[89Mol] used high-purity Ti wire, iodide Zr, and electrolytic Ni (99.9 mass% pure) to prepare arc melted alloys of $Ni(Ti,Zr)_2$ compositions. The alloys were annealed at 697 °C for 200 h and phase boundaries were determined with XRD and microscopy; DTA was used to determine liquid → solid transition temperatures. An isopleth (Fig. 5) shows the existence of an $MgZn_2$-type Laves phase (Ψ) around the composition NiTiZr. At 700 °C, the width of the Ψ phase region was reported to be between ~21 and 30 at.% Zr and the Ψ phase was shown to melt congruently at 920 °C near ~30 at.% Zr. On the other hand, [92Ere], who investigated the Ti-TiNi-NiZr-Zr composition region in greater detail (discussed later), also determined the $NiTi_2$-$NiZr_2$ isopleth using DTA and alloys annealed at 700 °C for 125 h and found (Fig. 6) that at 700 °C the Ψ phase exists between ~21 and 32 at.% Zr, but does not melt congruently. Moreover, on either side of the Ψ phase region no simple eutectic-type reactions occur. Since both [89Mol] and [92Ere] used component metals of high purity, the reason for this difference in the two reports of phase equilibrium in the $NiTi_2$-$NiZr_2$ system is uncertain. It is, however, noticed that the melting points of $NiTi_2$ and $NiZr_2$ phases determined by [89Mol] do not agree with the accepted values [91Nas]. Since [92Ere] made a more thorough study of the Ti-TiNi(β′)-NiZr(ϕ)-Zr region and reported a liquidus-solidus maximum at

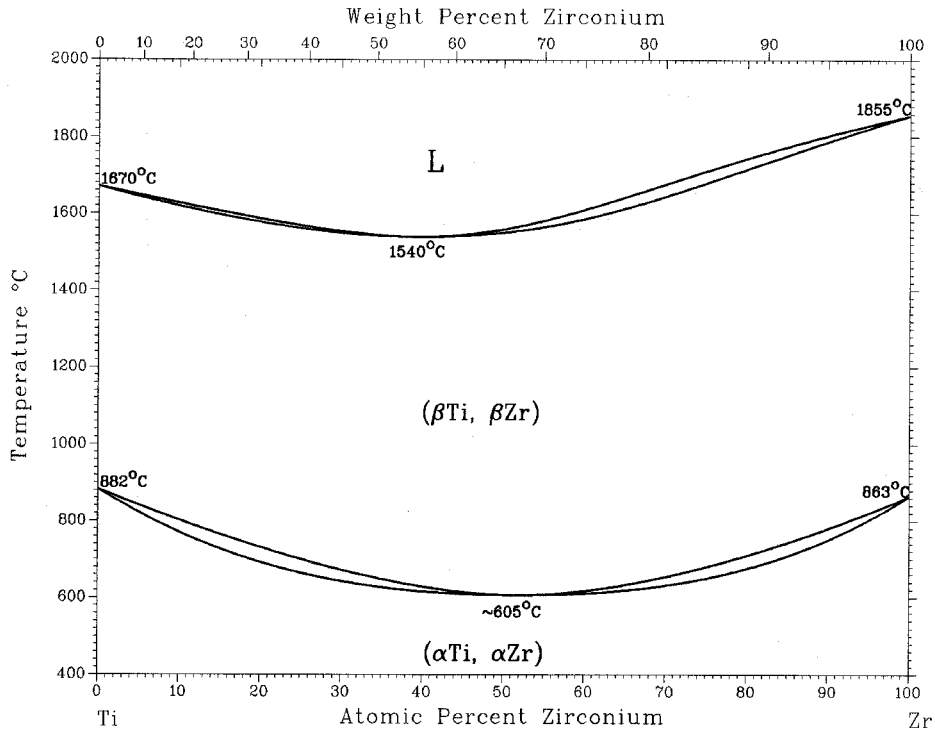

Fig. 3 Ti-Zi binary phase diagram [Massalski2]

~40 at.% Ti, 38 at.% Ni, and 22 at.% Zr, congruent melting of the Ψ phase [89Mol] does not appear to be probable. Further study of the melting of the Ψ phase in the $NiTi_2(\pi')$-$NiZr_2(\xi)$ system is desirable.

Isothermal Section

[88Ere] determined a 700 °C isothermal section for the composition region Ti-TiNi-NiZr-Zr (Fig. 7). Arc melted alloys were annealed stepwise from 950 → 800 → 700 °C (time of anneal not given), and phase analysis of annealed alloys was done with XRD, microscopy, and local x-ray spectroscopic analysis. A $MgZn_2$-type ternary Laves phase Ψ was found around the composition NiTiZr. The Ψ phase extends from ~14 to ~34 at.% Zr and from ~ 25 to ~39 at.% Ni. The Ψ phase was found in equilibrium with all the binary phases of the investigated composition region, namely $NiTi_2(\pi')$, NiTi(β′), NiZr(ϕ), $NiZr_2(\xi)$, and bcc(Ti,Zr) α solid solution. Five three-phase equilibrium triangles were established through local x-ray spectroscopic analysis (EPMA) of the phases. The compositions of phases in equilibrium are given in Table 2. Except near the Ti and Zr ends, the solid solubility of Ni in the α phase was found to be ~1 at.%. The extensions of the binary phases into the ternary were found to be ~5 at.% Ti for both the NiZr(ϕ) and $NiZr_2(\xi)$ phases and ~9 at.% Zr for the π′ phase. The phase equilibrium with the cph (Ti,Zr) ω phase was not determined and is shown in Fig. 7 in dashed lines to show the expected phase equilibrium.

Liquidus Projection

The NiTi-NiZr pseudobinary divides the Ni-Ti-Zr system into two parts. For the composition region with 0 to 50 at.% Ni, the course of crystallization of Ni-Ti-Zr alloys was studied by [91Ere1] and [92Ere]. The liquidus projection for the region <50 at.% Ni is given in Fig. 8, which also shows the composi-

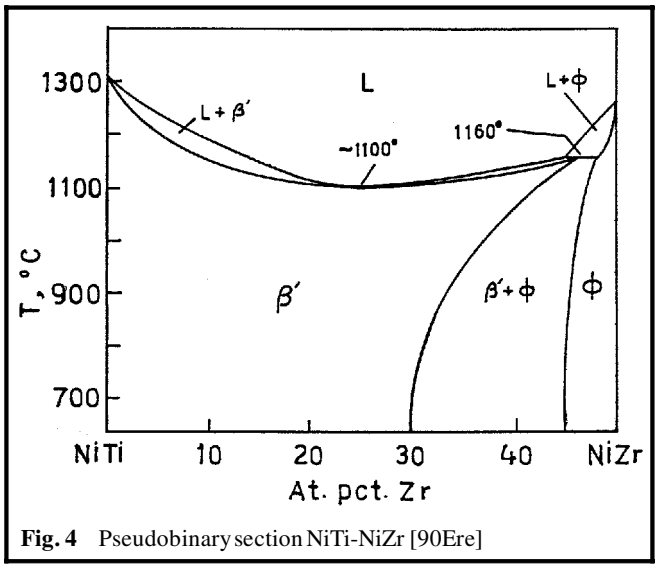

Fig. 4 Pseudobinary section NiTi-NiZr [90Ere]

Table 2 Composition of phases in three-phase equilibrium at 700 °C

Three-phase region	Phases in equilibrium	Composition, at.% Ni	Ti	Zr
α + π′ + Ψ	α	4.5	88.5	7.0
	π′	31.0	62.0	7.0
	Ψ	27.0	59.0	14.0
α + Ψ + ξ	α	1.5	30.5	68.0
	Ψ	28.0	36.0	34.0
	ξ	32.0	6.0	62.0
π′ + β′ + Ψ	π′	34.0	57.0	9.0
	β′	48.5	44.5	7.0
	Ψ	36.0	49.0	15.0
ϕ + Ψ + β′	ϕ	49.5	5.0	45.5
	Ψ	38.0	34.0	28.0
	β′	49.5	30.0	20.5
ϕ + Ψ + ξ	ϕ	49.0	1.0	50.0
	Ψ	34.0	33.0	33.0
	ξ	33.0	5.0	62.0

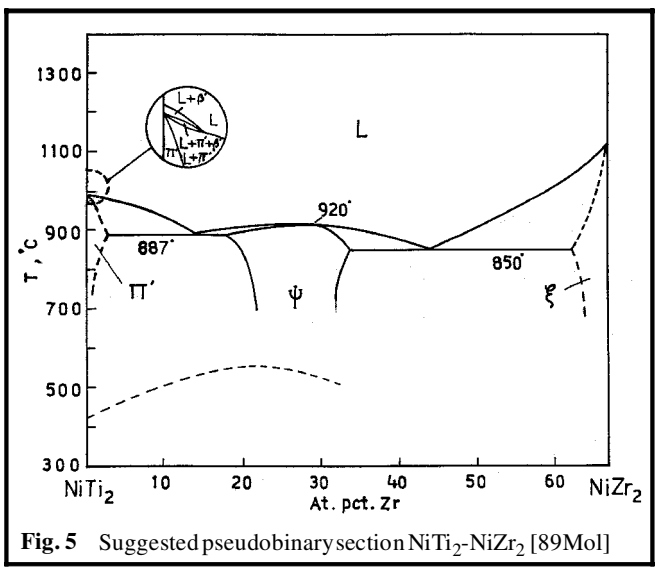

Fig. 5 Suggested pseudobinary section $NiTi_2$-$NiZr_2$ [89Mol]

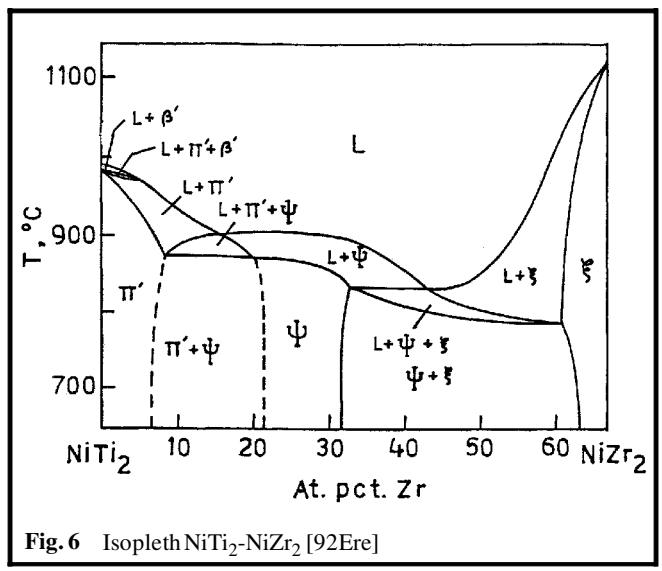

Fig. 6 Isopleth $NiTi_2$-$NiZr_2$ [92Ere]

tion of solids in equilibrium with liquid. The liquidus projection is characterized by rather flat liquidus and solidus surfaces [92Ere] and, at 925 °C, a reaction marked X in Fig. 8 [91Ere1] and [92Ere] suggesting liquid (L) in equilibrium with both Ψ and β′ phases with the same composition of L and Ψ phases of 39 at.% Ni and 22 at.% Zr, that is, a sort of critical tie-line with L and Ψ phases of the same composition in equilibrium with the β′ phase. The alloy containing 39 at.% Ni and 22 at.% Zr in the as-cast condition, however, shows a microstructure with primary β′ phase and a mixture of (β′ + Ψ) phases [91Ere1]. The presence of primary β′ phase in a cast alloys indicates that the liquidus surface is slightly above the invariant reaction

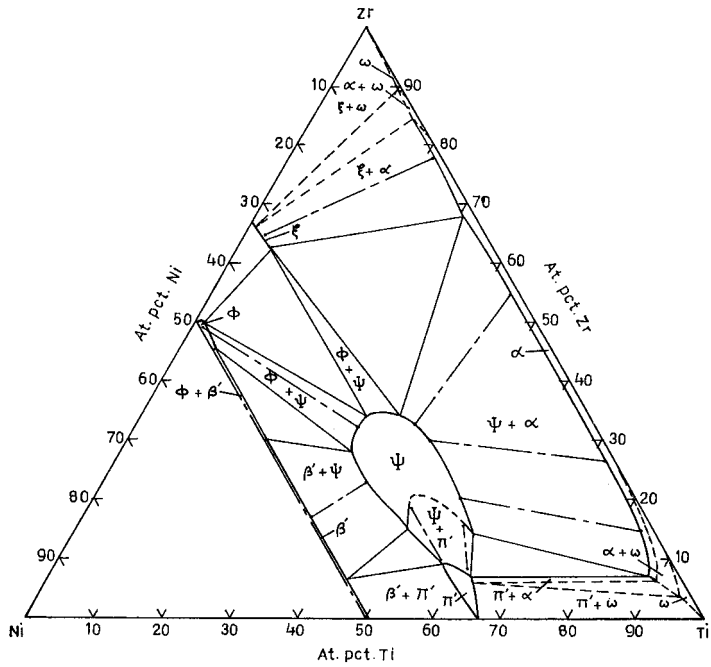

Fig. 7 A partial isothermal section of the Ni-Ti-Zr system at 700 °C in the composition region of 0 to 50 at.% Ni [88Ere]

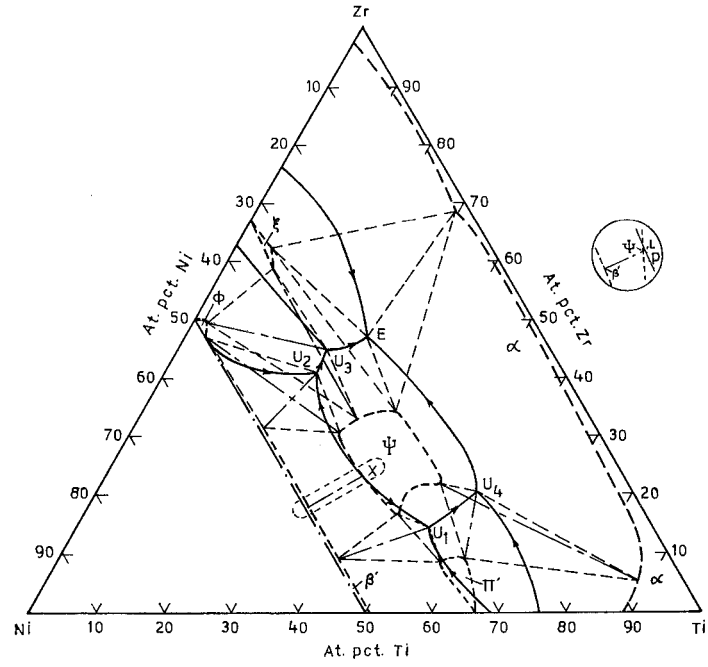

Fig. 8 Partial liquidus projection of the Ni-Ti-Zr system in the composition region of 0 to 50 at.% Ni. The compositions of the solid phases in equilibrium with liquid are also shown in thick dashed lines, and the four-phase equilibrium planes are shown in thin dashed lines [91Ere1, 92Ere]. The probable reaction for X is given within the circle.

temperature of 925 °C. The invariant reaction thus appears to be a peritectic-type reaction $L + \beta' \leftrightarrow \Psi$ with liquid composition very close to the peritectic composition. This interpretation of the available data requires verification through careful experimentation.

A partial reaction scheme for the Ni-Ti-Zr system is given in Fig. 9, in which the reaction at 925 °C is shown as a peritectic reaction. From the invariant reaction at 925 °C, the liquid composition changes toward the low Zr and toward the high Zr side to give two U-type reactions, U1: $L + \beta' \leftrightarrow \pi' + \Psi$ at 880

Table 3 Composition of phases in four-phase equilibrium at 700 °C

Reaction type	Equilibrium reaction	Invariant temperature, °C	Phases in equilibrium	Composition, at.% Ni	Ti	Zr
X(a)	…	925	L	39	38	23
			β'	49	34	17
			Ψ	23	38	39
U_1	$L + \beta' \leftrightarrow \pi' + \Psi$	880	L	33	53	14
			β'	49	44	7
			π'	34	58	8
			Ψ	37	47	16
U_2	$L + \beta' \leftrightarrow \Psi + \phi$	880	L	36	23	41
			β'	49	20	31
			Ψ	38	32	30
			ϕ	49	4	47
U_3	$L + \phi \leftrightarrow \Psi + \xi$	830	L	33	22	45
			ϕ	49	2	49
			Ψ	33	34	33
			ξ	33	7	60
U_4	$L + \pi' \leftrightarrow \Psi + \alpha$	810	L	23	57	20
			π'	31	60	9
			Ψ	28	50	22
			α	4.5	87.9	7.6
E	$L \leftrightarrow \Psi + \alpha + \xi$	770	L	26	27	47
			Ψ	29	38	33
			α	1.5	29.5	69
			ξ	32	6	62

(a) The reaction is possibly peritectic type $L + \beta' \leftrightarrow \Psi$.

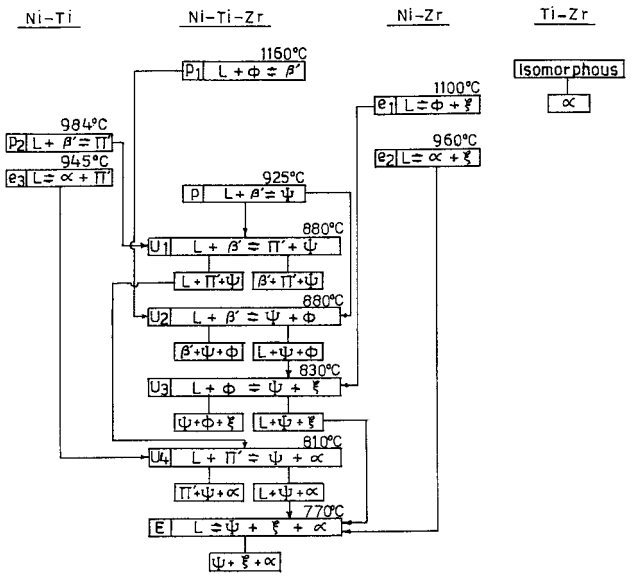

Fig. 9 Reaction scheme for the composition region of 0 to 50 at.% Ni [91Ere1, 92Ere]

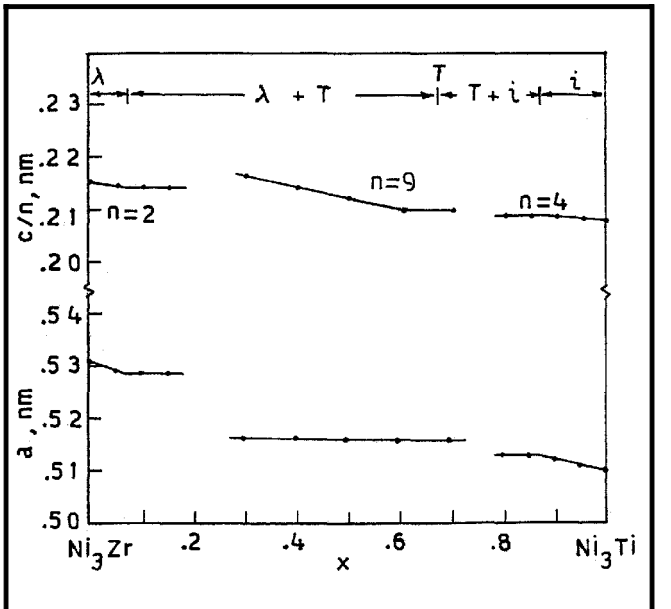

Fig. 10 Variation of lattice parameters of the Ni_3Zr (λ), T, and Ni_3Ti(ι) phases along the $Ni_3(Ti_xZr_{1-x})$ composition line [87Gli]

°C and U2: L + β′ ↔ Ψ + ϕ at 880 °C and then two more U-type reactions occur, U3: L + ϕ ↔ Ψ + ξ at 830 °C and U4: L + π′ ↔ Ψ + α at 810 °C. Finally, the last liquid solidifies through an E-type reaction, E: L ↔ α + Ψ + ξ at 770 °C. The compositions of phases in various four-phase reactions are given in Table 3.

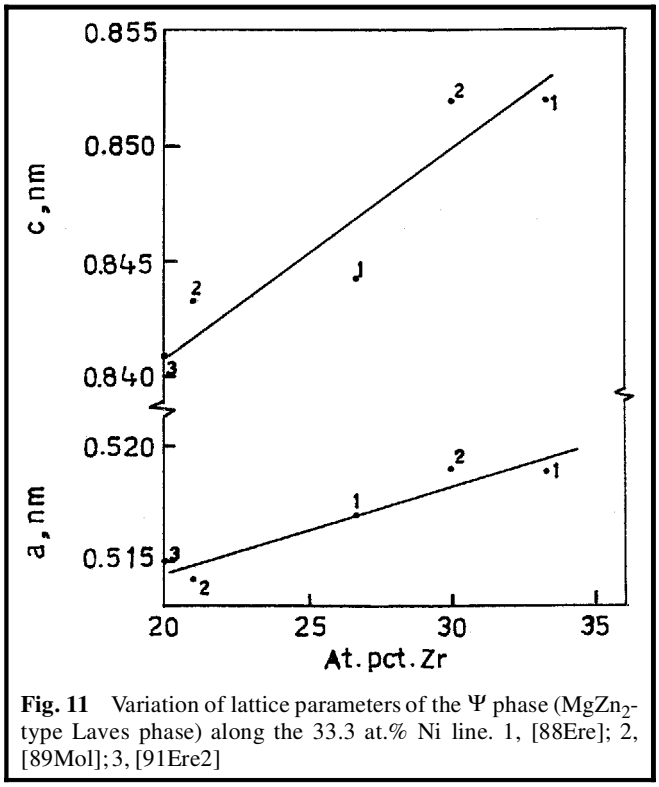

Fig. 11 Variation of lattice parameters of the Ψ phase ($MgZn_2$-type Laves phase) along the 33.3 at.% Ni line. 1, [88Ere]; 2, [89Mol]; 3, [91Ere2]

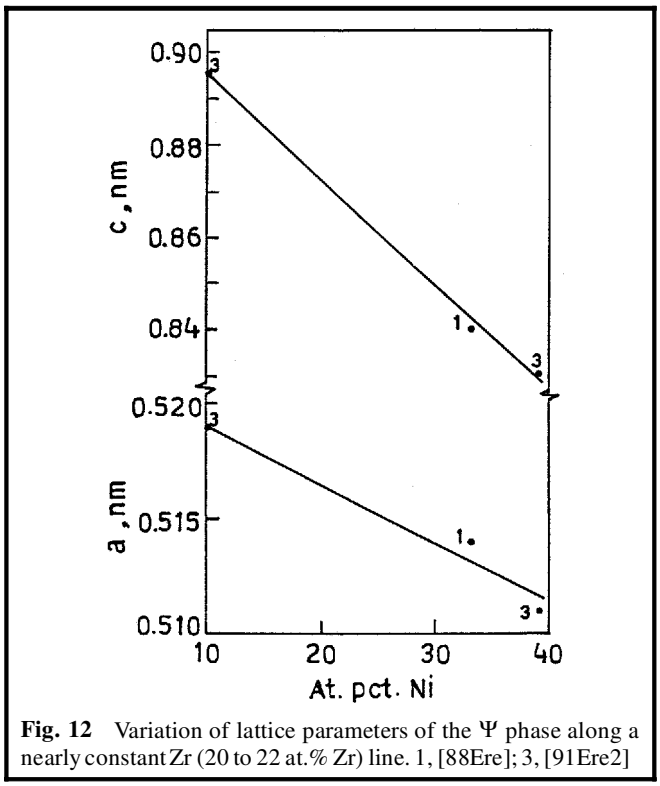

Fig. 12 Variation of lattice parameters of the Ψ phase along a nearly constant Zr (20 to 22 at.% Zr) line. 1, [88Ere]; 3, [91Ere2]

Lattice Parameters

[87Gli] determined lattice parameters of the $Ni_3(Ti_xZr_{1-x})$ and reported lattice parameters as a function of Ti content for the Ni_3Zr(λ), Ni_3Ti(ι), and Ni_3(Ti,Zr)T phases (Fig. 10). Like many AB_3-type phases, the λ, ι, and T phase structures can be correlated in terms of atomic layer stackings: the λ phase has a sequence of two-layer stackings, *AB*, the ι phase has a four-layer stacking *ABAC*, and the T phase has a nine-layer stacking *ABABCBCAC*. In Fig. 10 [87Gli] plots for the *c* parameter *c*/*n*, where *n* = 2, 4, and 9. The results indicate a decrease in lattice parameters for the λ and ι phases with increase in Ti content, whereas for both sides of T phase (*x* = 0.6 and *x* = 0.7), the lattice parameter of the T phase was found to be the same. Surprisingly, however, [87Gli] found the *c* parameter of the T phase to increase in the two-phase region of λ + T with increase in Zr content. This suggests that there may be other AB_3-type phases between the T and λ phases. The $Ni_3(Ti_xZr_{1-x})$ alloys should be reinvestigated in the λ + T region to determine the cause of monotonic increase of the *c* parameter of the T phase.

Lattice parameters of the Ψ phase were reported by various investigators. The available lattice parameter data have been used to indicate the variations of the Ψ phase lattice parameters as a function of composition for constant Ni content (33.3 at.% Ni) and for approximately constant Zr (20 to 22 at.%) contents, respectively, in Fig. 11 and 12. As expected, the lattice parameters were found to increase with increase in Zr content and decrease with increase in Ni content.

Even though [89Ere] established the pseudobinary NiTi-NiZr and observed a wide β′ phase field, the lattice parameter for the whole range of stability of the β′ phase was not reported. Using the reported lattice parameters of the β′ phase by different investigators, the variation of lattice parameter of the β′ phase as a function of Zr content has been plotted and given in Fig. 13. The lattice parameter of the β′ phase increases with increase in Zr content.

For the $NiTi_2$(π′) and $NiZr_2$(ξ) phases, the lattice parameters reported by [88Ere] are *a* = 1.133 nm, *a* = 0.649 nm, and *c* = 0.527 nm, respectively, which are close to the values given

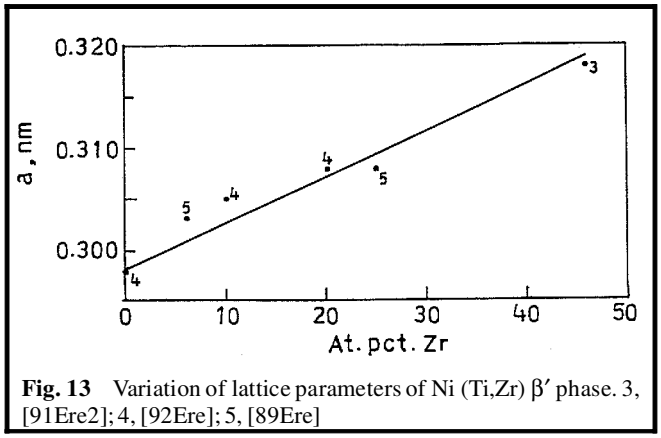

Fig. 13 Variation of lattice parameters of Ni (Ti,Zr) β′ phase. 3, [91Ere2]; 4, [92Ere]; 5, [89Ere]

by [Pearson] (see Table 1). The π' and ξ phases extend into the ternary only slightly. [91Ere2] reported the lattice parameters of the π' phase, of composition 33 at.% Ni and 5 at.% Zr, and ξ phase, of composition 33 at.% Ni and 4.2 at.% Ti, as a = 1.137 nm and a = 0.648 nm, and c = 0.524 nm, respectively.

Amorphous Alloys

Through DTA of melt-spun amorphous $Ni(Ti_xZr_{1-x})_2$ alloys, [89Mol] showed crystallization temperature to go through a maximum of 542 °C between 20 and 22 at.% Zr (Fig. 5). At ~50 at.% Zr two thermal effects of equal intensity observed at 390 and 480 °C electrical resistivity of the amorphous alloys decreased from 222 μΩ cm at the $NiTi_2$ end to 168 μΩ cm at the $NiZr_2$ end.

A further study was made by [88Sib] to detect the presence of icosahedral phase in melt-spun $Ni_{20}(Ti,Zr)_{80}$ alloys. The icosahedral phase was found over a wide composition range of 20 to 60 at.% Zr, the terminal phases did not produce icosahedral phase. The alloy $Ni_{20}Ti_{53.5}Zr_{26.5}$ with melting point 840 °C was studied in more detail. For melt-spun tapes, ≤80 μm, only icosahedral phase was found, but in >100 μm tapes icosahedral phase together with Ψ phase existed. Electrical resistivity was 185 μΩ cm, and crystallization temperature was 695 °C. The icosahedral phase, similar to that found in Mg-Al-Zn and Ga-Mg-Zn, but different from that in Al-Mn system, could be removed only after three cycles of heating and cooling between room temperature and 727 °C. On crystallization the icosahedral phase changes to the Ψ phase. The activation energy of phase transformation was estimated to be ~5.5 ev/atom.

Acknowledgment

The author wishes to acknowledge the financial support provided by the Department of Science and Technology, Government of India, New Delhi, for the evaluation of nickel and cobalt ternary systems.

References

66Vuc: J.H.N. van Vucht, Influence of Radius Ratio on the Structure of Intermetallic Compounds of the AB_3 Type, *J. Less Common Met.,* Vol 11, 1966, p 308-322. (Experimental)

87Gli: J.L. Glimois, P. Forey, R. Guillen, and J.L. Feron, Structural Study of the Ternary Alloys $(Ti_xZr_{1-x})Ni_3$, *J. Less Common Met.,* Vol 134, 1987 p 221-228. (Experimental)

***88Ere:** V.N. Eremenko, E.L. Semenova, and L.A. Tretyachenko, The Structure of Ni-Zr-Ti Alloys in the Region of 0-50% Ni at 700 °C, *Dop. Akad. Nauk Ukr. RSR, Fiz. Met. Tekh.* (No. 2), 1988, p 76-79 (in Russian). (Experimental,#)

88Sib: S.A. Sibrirlsev, V.N. Chebotnikov, V.V. Molokanov, and Yu.K. Kovneristyi, Quasicrystals in the Ti-Zr-Ni System, *JETP Lett.,* Vol 47 (No. 12), 1988, p 744-746. (Experimental)

***89Mol:** V.V. Moloknov, V.N. Chebotnikov, and Yu.K. Kovneristyi, The Structure and Properties of Alloys of the Cross Section Ti_2Ni-Zr_2Ni of the System Ti-Ni-Zr in the Amorphous and Crystalline State, *Izv. Akad. Nauk SSSR, Neorganic. Mater.,* Vol 25 (No. 1), 1989, p 61-65 (in Russian). (Experimental,#)

***90Ere:** V.N. Eremenko, E.L. Semenova, L.A. Tretyachenko, and Z.G. Domatyrko, Constitution of the Ternary Ni-Zr-Ti Alloys along the TiNi-ZrNi Section, *Izv. V.U.Z. Tsvetn. Metall.* (No. 6), 1990, p 85-88 (in Russian). (Experimental,#)

***91Ere1:** V.N. Eremenko, E.L. Semenova, and L.A. Tretyachenko, Liquidus Surface and Solidification Scheme for Alloys of the System Ti-Ni-Zr Containing up to 50% Ni, *Poroshk. Metall.* (No. 8), 1991, p 49-54 (in Russian). (Experimental,#)

***91Ere2:** V.N. Eremenko, E.L. Semenova, and L.A. Tretyachenko, Projection of the Solidus Surface of the Ternary System Ti-Ni-Zr in the Region Ti-TiNi-ZrNi-Zr, *Dokl. Akad. Nauk SSSR, Metall.* (No. 6), 1991, p 191-196 (in Russian). (Experimental,#)

91Nas: P. Nash, *Phase Diagrams of Binary Nickel Alloys,* ASM International, 1991. (Review)

***92Ere:** V.N. Eremenko, E.L. Semenova, and L.A. Tretyachenko, Projection of the Solidus Surface and Reactions During Solidification of Ti-Ni-Zr Alloys in the Ti-TiNi-ZrNi-Zr Region, *Russ. Akad. Nauk Metall.* (No. 6), 1992, p 138-143 (in Russian). (Experimental,#)

*Indicates key paper.

#Indicates presence of a phase diagram.

Ni-Ti-Zr evaluation contributed by **K.P. Gupta,** The Indian Institute of Metals, Metal House, Plot 13/4, Block AQ, Sector V, Calcutta, India. Literature searched through 1993. Dr. Gupta is the Alloy Phase Diagram Program Co-Category Editor for ternary nickel alloys.